Acta Crystallographica Section D
Biological Crystallography
ISSN 0907-4449

Structural and pharmacological comparison of daboiatoxin from *Daboia russelli siamensis* with viperotoxin F and vipoxin from other vipers

Gayathri Gopalan,[a]‡§ Maung-Maung Thwin,[b]§ Ponnampalam Gopalakrishnakone[b] and Kunchithapadam Swaminathan[a,c]*

[a]Department of Biological Sciences, National University of Singapore, Singapore 117543, Singapore, [b]Department of Anatomy, National University of Singapore, Singapore 117543, Singapore, and [c]Institute of Molecular and Cell Biology, 61 Biopolis Drive, Singapore 138673, Singapore

‡ Current address: Department of Chemistry and Biochemistry, Arizona State University, Tempe, Arizona 85287-1604, USA.
§ These authors contributed equally to this work.

Correspondence e-mail: dbsks@nus.edu.sg

Received 9 December 2006
Accepted 2 April 2007

PDB Reference: daboiatoxin, 2h4c, r2h4csf.

Russell's viper (*Vipera russelli*, also known as *Daboia russelli*) is one of the major causes of fatal snakebites. To date, five *Daboia russelli* subspecies have been recognized. Daboiatoxin (DbTx) is the main lethal phospholipase A_2 (PLA_2) toxin in the venom of *D. russelli siamensis* (Myanmar viper) and has strong neurotoxic, myotoxic and cytotoxic activities. DbTx and its homologous neurotoxins viperotoxin F from *D. russelli formosensis* (Taiwan viper) and vipoxin from the Bulgarian sand viper *V. ammodytes meridionalis* consist of complexes between a nontoxic acidic PLA_2 protein and an enzymatically active basic PLA_2. DbTx and viperotoxin F are presynaptic toxins, while vipoxin is postsynaptic. The two chains of DbTx have been separated and their PLA_2 enzymatic activity has been measured using the secretory PLA_2 assay kit. The enzymatic activity of DbTx chain B is reduced by 30% of its original activity by chain A in a unimolar ratio, thus indicating that DbTx chain A acts as an inhibitor. The lethal activity of the two chains has also been studied in male albino mice and chain A is less lethal than chain B. The crystal structure of DbTx has also been determined and its structural details are compared with those of the two homologues. Furthermore, an attempt is made to correlate the sequence and structural determinants of these toxins with their enzymatic activities and their pharmacological effects.

1. Introduction

Russell's viper (*Vipera russelli*, also known as *Daboia russelli*) is one of the major causes of fatal snakebites in Southeast Asia, resulting in more than 1000 deaths annually (Thwin *et al.*, 1995). Clinical studies of *D. russelli* bites have confirmed a geographical variation in venom composition, with symptomatology varying with locality (Warrell *et al.*, 1989). To date, five *Daboia russelli* subspecies have been recognized: *D. russelli russelli* (Indian viper), *D. russelli pulchella* (Sri Lankan viper), *D. russelli siamensis* (Thailand and Myanmar vipers), *D. russelli formosensis* (Taiwan viper) and *D. russelli limitis* (Indonesian viper) (Wuster *et al.*, 1992). The phospholipase A_2 (PLA_2) enzyme (EC 3.1.1.4) is one of the most toxic constituents of snake venoms. Despite having very high sequence homology, PLA_2s generally exhibit a large variations in their pharmacological activities (Lok *et al.*, 2005). Several isoforms (Huang & Lee, 1984) are known to be present in almost all *D. russelli* venoms (VRVs or DRVs). A variety of PLA_2 toxins (VRV PL-V, VRV PL-VI, VRV PL-VIIIa and daboiatoxin) with molecular weights ranging from 10 to 16 kDa have been isolated from DRVs (Thwin *et al.*, 1995). They exhibit a wide variety of pharmacological and physiopathological effects, including neurotoxicity, myotoxicity, haemostatic disturbance, haemolysis, cardiotoxicity and hypotension (Warrell, 1989).

In general, two major types of DRVs have been reported. The first type includes the type N venoms (*D. russelli formosensis*, *D. russelli siamensis* and *D. russelli russelli*), which are PLA_2s with an N-terminal asparagine residue, while the second type includes the type S venoms (*D. russelli pulchella*), which are PLA_2s with an N-terminal serine residue (Tsai *et al.*, 1996). It is interesting to note that the PLA_2 sequences of *D. russelli siamensis* (Thailand) are more homologous to those of *D. russelli formosensis* than to those of daboiatoxin from *D. russelli siamensis* (Myanmar), which indicates great variation even among venoms from the same subspecies (Thwin *et al.*, 1995; Tsai *et al.*, 1996).

Daboiatoxin (DbTx) is the main lethal PLA_2 toxin in the venom of *D. russelli siamensis* (Myanmar viper) and has strong neurotoxic, myotoxic and cytotoxic activities. It also has oedema-inducing and indirect haemolytic activity, but lacks haemorrhagic activity. It exists as a heterodimer of two PLA_2 chains (DbTx-A and DbTx-B). Sequence similarity has been noted between DbTx of *D. russelli siamensis* (Myanmar viper), viperotoxin F from *D. russelli formosensis* (Taiwan viper) and the vipoxins from the Bulgarian sand vipers *V. ammodytes meridionalis* and *V. ammodytes ammodytes* (Fig. 1). The heterodimeric neurotoxin viperotoxin F (28 kDa RV-7–RV-4 complex) represents a complex between a nontoxic acidic PLA_2 (RV-7, equivalent to DbTx-A) and RV-4, a neurotoxic and enzymatically active basic PLA_2 (equivalent to DbTx-B; Wang *et al.*, 1992), which has 100-fold higher hydrolytic activity than RV-7. Vipoxin is also a similar heterodimeric complex of an acidic PLA_2-like natural inhibitor and a basic highly toxic PLA_2 (Mancheva *et al.*, 1987). Unlike DbTx-A and RV-7, the inhibitor chain of vipoxin is completely inactive. DbTx and viperotoxin F are presynaptic toxins, while vipoxin is postsynaptic (Mancheva *et al.*, 1987; Thwin *et al.*, 1996). Despite this marked difference in their pharmacological properties, the sequences of RV-7 and RV-4 are 92% identical to those of the two corresponding components of the vipoxin complex (Table 1). The RV-7–RV-4 complex has accordingly been suggested as a structural analogue of DbTx and vipoxin (Perbandt *et al.*, 2003).

Table 1
Homology between DbTx (inhibitor DbTx-A and active DbTx-B) of *D. russelli siamensis* (Myanmar viper), viperotoxin F (inhibitor RV-7 and active RV-4) from *D. russelli formosensis* (Taiwan viper) and vipoxin from the Bulgarian sand viper *V. ammodytes meridionalis* (inhibitor MER-INH and active MER-PLA_2).

Sequence 1	Sequence 2	Homology (%)
DbTx-A	DbTx-B	60
RV-7	RV-4	65
MER-INH	MER-PLA_2	63
DbTx-A	RV-7	88
DbTx-A	MER-INH	84
RV-7	MER-INH	92
DbTx-B	RV-4	68
DbTx-B	MER-PLA_2	68
RV-4	MER-PLA_2	91

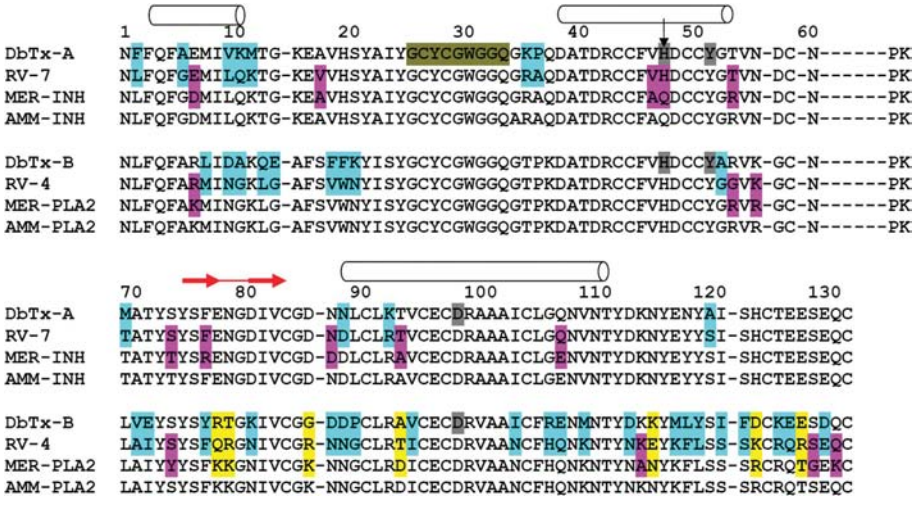

Figure 1
Sequence alignment of DbTx, viperotoxin F and vipoxin. The sequences are from DbTx (inhibitor DbTx-A and active DbTx-B) from *D. russelli siamensis* (Myanmar viper), viperotoxin F (RV-7 and RV-4) from *D. russelli formosensis* (Taiwan viper) and the vipoxins from the Bulgarian vipers *V. ammodytes meridionalis* (MER-INH and MER-PLA_2) and *V. ammodytes ammodytes* (AMM-INH and AMM-PLA_2, not used for alignment). Nonmatching residues for all three sequences are highlighted in yellow. Nonmatching residues between DbTx and RV are highlighted in blue. The differences between RV and MER are highlighted in magenta; note that the corresponding DbTx residue matches one of them. The secondary-structure elements of DbTx are shown above its sequence. α-Helices are shown as cylinders and the β-strands of the β-wing of DbTx are shown as red arrows. The amino acids of the calcium-binding loop are highlighted in dark yellow. The catalytic amino acids His48, Tyr52 and Asp99 of DbTx are highlighted in grey. The difference in amino acids at position 48 is indicated by a vertical black arrow. The amino-acid numbering scheme follows that of Renetseder *et al.* (1985). See Table 1 for the percentage homologies between these sequences.

The crystal structures of the viperotoxin F complex from *D. russelli formosensis* (Perbandt *et al.*, 2003), the vipoxin complexes from *V. ammodytes meridionalis* (Perbandt *et al.*, 1997) and *V. ammodytes ammodytes* (Banumathi *et al.*, 2001) and PLA_2 from *D. russelli pulchella* (Chandra *et al.*, 1999, 2000, 2001) have been reported. However, there is no structural information available on the PLA_2s of *D. russelli siamensis*. Here, we report the crystal structure of daboiatoxin (containing the DbTx-A and DbTx-B chains) isolated from the venom of *D. russelli siamensis*, which is mainly found in Myanmar. Also, we interpret how the structural and sequence differences between DbTx, viperotoxin F and vipoxin are reflected in the activity and pharmacological behaviour of these toxins.

2. Materials and methods

2.1. Purification of the DbTx complex and component chains

The lyophilized venom of *D. russelli siamensis* was purified by a two-step process consisting of size-exclusion and

anion-exchange chromatography. 100 mg crude venom was dissolved in 50 m*M* phosphate buffer pH 7.0 to a concentration of 25 mg ml^{-1} and centrifuged at 10 000*g* for 20 min to remove all insoluble matter. The supernatant was loaded onto a Superdex 75 gel-filtration column (Amersham Pharmacia) pre-equilibrated with 50 m*M* phosphate buffer pH 7.0 at 293 K. The fractions that contained proteins with molecular weight of around 30 kDa and showed PLA_2 activity were pooled and loaded onto a UNO-Q (Amersham Pharmacia) anion-exchange column (6 × 2.0 cm) pre-equilibrated with 50 m*M* sodium acetate buffer pH 5.0. The protein of interest was eluted using a linear salt gradient of 0–0.5 *M* NaCl in 50 m*M* sodium acetate buffer pH 5.0. The peak in the final elution profile was confirmed to be PLA_2 by SDS–PAGE, activity assay, mass spectrometry and N-terminal amino-acid sequencing. The purified complex of DbTx (DbTx-A and DbTx-B heterodimer) was concentrated to 10 mg ml^{-1} and stored at 193 K.

DbTx contains two strongly associated PLA_2 chains in both the crystal and in solution (even at very low concentrations). This was confirmed by reverse-phase high-performance liquid chromatography (RP-HPLC) and dynamic light scattering

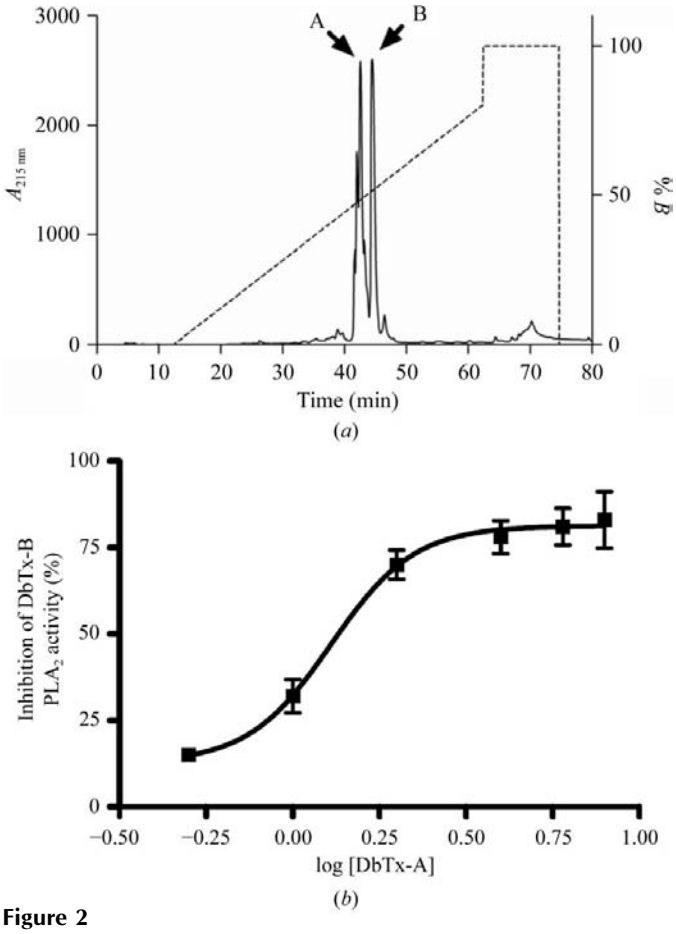

Figure 2
Separation of subunits and activity of DbTx. (*a*) Reverse-phase HPLC profile of the DbTx-A inhibitor and DbTx-B PLA_2 subunits. The elution positions of DbTx-A and DbTx-B subunits are marked by arrows and the percentage of buffer *B* in the elution gradient is marked by a dashed line. (*b*) The activity of the DbTx-B PLA_2 chain is quenched by the DbTx-A inhibitor chain.

Table 2
Crystal parameters and data-collection and refinement statistics for the DbTx structure.

Values in parentheses are for the highest resolution shell (2.69–2.60 Å).

Crystal parameters	
Space group	$P3_2$
Unit-cell parameters	
a (Å)	67.0
c (Å)	240.3
No. of molecules in ASU	4 (8 PLA_2s)
Matthews coefficient V_M (Å^3 Da^{-1})	2.78
Solvent content (%)	56.0
Data collection	
X-ray source	NSLS beamline X12B
Detector	ADSC Q315 CCD
Resolution (Å)	2.6
Total observations	224250
Unique reflections	53393
Completeness (%)	99.3 (100.0)
Redundancy	4.2 (4.1)
R_{sym}†	0.074 (0.164)
Refinement	
Resolution range (Å)	8.0–2.6
Reflections (working/test)	30637/3169
R_{cryst}‡ [with $\|F_o\| > 0\sigma(\|F_o\|)$]	0.220
R_{free}	0.307
Non-H atoms	7680
Waters	199
Average *B* factors (Å^2)	
Protein	36.6
Water	30.0
R.m.s.d. in bond lengths (Å)	0.023
R.m.s.d. in bond angles (°)	1.5

† $R_{sym} = \sum_{hkl}\sum_i[I_i(hkl) - \langle I(hkl)\rangle|/\sum_{hkl}\sum_i I_i(hkl)]$. ‡ *R* factor = $\sum_{hkl}\big||F_o(hkl)| - |F_c|\big|/\sum_{hkl}|F_o(hkl)|$.

(DLS). The results of DLS showed that the mean hydrodynamic radius (R_h) of DbTx is 2.45 nm. The molecular weight corresponding to this hydrodynamic radius was estimated to be 28 kDa. Furthermore, the gel-filtration profile also indicated a molecular weight of 28 kDa. Thus, the above results clearly show that the two subunits of DbTx exist bound together in the solution state.

The A and B subunits of DbTx were separated from the DbTx dimeric complex using an AKTA Explorer 100 High Performance Liquid Chromatography (HPLC) system (Amersham Pharmacia Biotech). 400 µg of the dimeric complex was loaded onto a Jupiter C_{18} reverse-phase column (250 × 4.6 mm; 10 µm; Phenomenex) equilibrated with solution *A* (0.1% TFA). Elution of the two subunits was effected by applying a 1 ml min^{-1} linear gradient from 0 to 75% solution *B* (80% acetonitrile in 0.1% TFA; Fig. 2*a*). The hydrodynamic radius of each subunit of DbTx was 1.54 nm, which corresponds to a molecular weight of 14 kDa.

2.2. X-ray crystallography

Crystals of the DbTx complex were first observed in a calcium chloride grid screen (Molecular Dimensions) using the sitting-drop vapour-diffusion method at 293 K. 2 µl protein solution (10 mg ml^{-1}) was mixed with 2 µl precipitant solution. After optimization, the following condition formed crystals suitable for X-ray diffraction studies: 1.5 *M* $CaCl_2$,

0.1 *M* Tris–HCl pH 9.0, 10%(*w*/*v*) PEG 4000. The rectangular complex crystals had average dimensions of 0.2 × 0.1 × 0.05 mm. Precipitant solution with 25% glycerol was used as a cryoprotectant for flash-freezing crystals in liquid nitrogen.

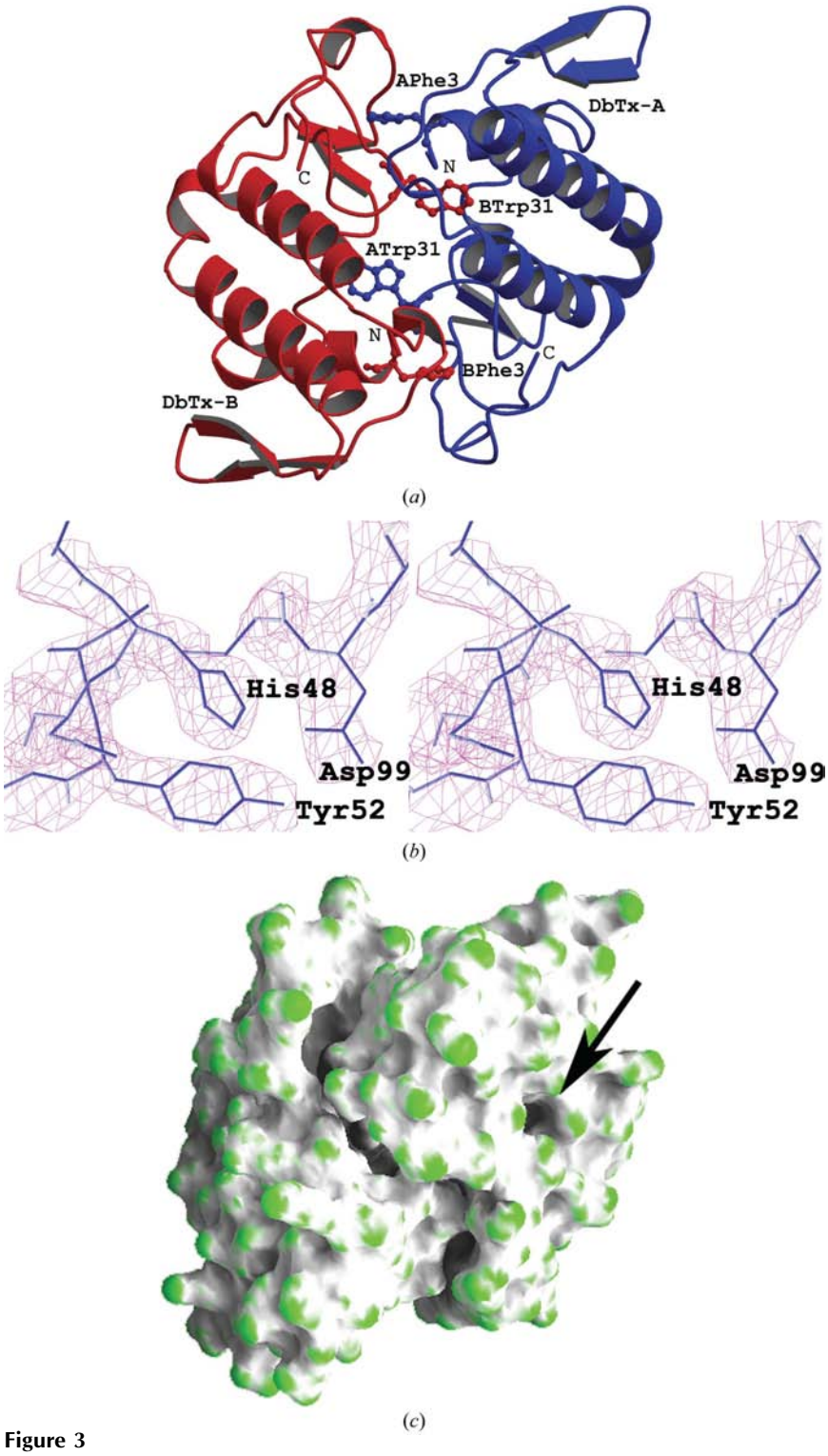

Figure 3
The three-dimensional structure and active site of DbTx. (*a*) The two PLA_2 chains in the heterodimer of DbTx are viewed down the local twofold axis. The Phe3 and Trp31 residues that regulate the hydrophobic tunnels in the DbTx molecule are shown. (*b*) Stereoview of the electron density in the vicinity of the active site for the inhibitor chain DbTx-A. This $2F_o - F_c$ map is contoured at the 1.3σ level. The catalytic triad residues are labelled. (*c*) Surface-curvature drawing of DbTx. The entrance of the hydrophobic tunnel for DbTx-A is pointed out by an arrow.

X-ray diffraction data were collected from the DbTx crystals using synchrotron radiation at National Synchrotron Light Source (USA) beamline X12B and were processed using *DENZO*, *HKL*-2000 and *SCALEPACK* (Otwinowski & Minor, 1997).

The structure of DbTx was determined by molecular replacement using *MOLREP* (Vagin & Teplyakov, 1997; Collaborative Computational Project, Number 4, 1994). The structure of the RV-7–RV-4 complex (PDB code 1oqs) was used as the initial search model for the DbTx structure. The crystals of DbTx were subsequently found to be hemihedrally twinned. Model building and refinement were carried out using *O* (Jones *et al.*, 1991) and *CNS* (Brünger *et al.*, 1998), respectively. All water molecules were located from difference Fourier maps with peak heights greater than 3σ. The accuracy of the model was confirmed from simulated-annealing OMIT maps and the geometry of the structure was assessed using *PROCHECK* (Laskowski *et al.*, 1993) and *WHAT_CHECK* (Hooft *et al.*, 1996). On average, only one amino acid per chain (of 122 amino acids) is located in the disallowed region of the Ramachandran plot. All molecular drawings were prepared using *MOLSCRIPT* (Kraulis, 1991) and *RASTER3D* (Merritt & Bacon, 1997). The details of data collection and refinement are given in Table 2.

2.3. PLA_2 catalytic activity

The catalytic activity of DbTx (individual subunits A and B, the dimeric complex and the complexes formed upon mixing the two subunits in various molar ratios) was determined using the secretory PLA_2 assay kit (Cayman Chemicals). The substrate used in this assay was the 1,2-dithio analogue of diheptanoyl phosphatidylcholine. The release of free thiols upon PLA_2-catalyzed hydrolysis of the thioester bond at the *sn*-2 position was detected spectrophotometrically using 5,5′-dithio-bis-(2-nitrobenzoic acid) (Fig. 2*b*).

3. Results

3.1. Overall structure

We have crystallized the complete daboiatoxin molecule (the complex between

the acidic DbTx-A chain and the basic DbTx-B chain) from *D. russelli siamensis* (Myanmar viper), which is the equivalent of viperotoxin F from *D. russelli formosensis* (Taiwan viper; Perbandt *et al.*, 2003) and the vipoxins from the Bulgarian sand vipers *V. ammodytes meridionalis* (Perbandt *et al.*, 1997) and *V. ammodytes ammodytes* (Banumathi *et al.*, 2001) (Fig. 1). Gel-filtration profiles and dynamic light-scattering (DLS) studies have indicated that the two chains are also associated in solution, even at low concentrations. The overall conformations of DbTx-A and DbTx-B are essentially similar and the two chains superimpose on each other with a root-mean-square deviation (r.m.s.d.) of 0.99 Å for the 122 C^{α} atoms (Fig. 3*a*). The corresponding value for superimposition of the equivalent RV-7 and RV-4 chains of viperotoxin F is 1.41 Å, whereas that for the inhibitor chain (MER-INH) and the active chain (MER-PLA_2) of vipoxin is 1.49 Å. The electron density is well defined throughout the molecule (Fig. 3*b*).

As expected, the overall fold and disulfide network in DbTx are similar to those in other known PLA_2s. However, there are three prominent regions that show significant conformational differences between the two chains; namely, the calcium-binding loop (including Trp31), the β-wing (consisting of two antiparallel β-strands) and the C-terminal residues. The long interface between the two PLA_2 chains is stabilized by several hydrogen bonds, one salt bridge and a number of hydrophobic interactions. A hydrophobic channel is formed by the generally invariant Leu2, Phe3, Ile9, Tyr22, Cys25, Cys45, Ala102 and Ala103 residues and aids in binding the substrate in PLA_2s. The hydrophobic channel in PLA_2s allows substrate molecules to reach the active centre. Several water molecules are buried at the bottom of the hydrophobic pocket, which is covered by the two Phe3 residues of the dimer. These water molecules are involved in a network of hydrogen bonds to main-chain O atoms and stabilize the overall conformation of DbTx.

This hydrophobic channel of DbTx extends to the interface between the subunits. It may be noted that Trp31 forms a lid for the hydrophobic channel and its orientation undergoes positional changes in order to close and open as a gate to the channel (Figs. 3*a* and 3*c*; Chandra *et al.*, 2001). These structural determinants are functionally relevant, with particular reference to the calcium-binding loop, which is intimately linked to the resulting conformation of the hydrophobic channel.

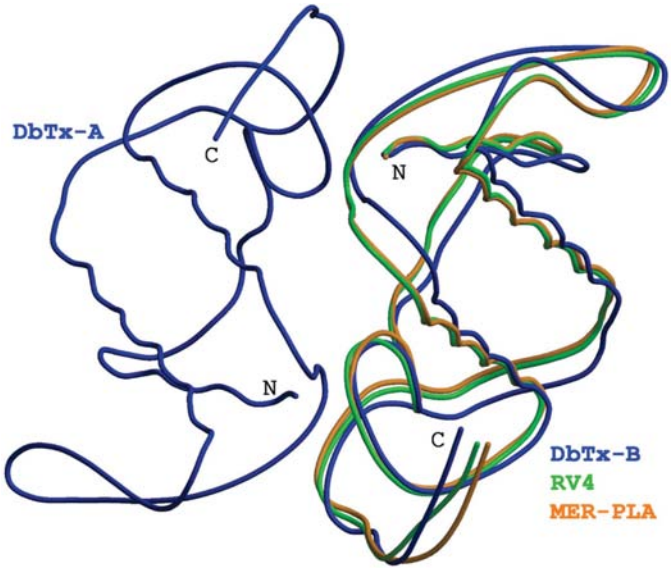

Figure 4
Superimposition of the backbones of DbTx from *D. russelli siamensis* (blue), viperotoxin F from *D. russelli formosensis* (green) and vipoxin from *V. ammodytes meridionalis* (orange). DbTx-A was used as reference and the equivalent chains of the other two structures were superimposed onto it. The three structures were aligned using the *MULTIPROT* server (Shatsky *et al.*, 2002).

3.2. Structural comparison of DbTx with viperotoxin F and vipoxin

DbTx and its homologues, the viperotoxin F and vipoxin complexes, contain two PLA_2 chains, one of which is an acidic and catalytically less active PLA_2-like natural inhibitor while the other is a basic and highly toxic PLA_2. The two chains of the heterodimer align through nearly exact twofold rotational symmetry (Fig. 3*a*) and superimpose well onto the corresponding viperotoxin F and vipoxin PLA_2 subunits (Fig. 4). However, the interface between the two subunits is stabilized by differing amounts of contact area and a different number of salt bridges in the three structures (Fig. 5).

DbTx superimposes with viperotoxin F and vipoxin with r.m.s.d. values of 1.25 and 1.39 Å, respectively, for 244 C^{α} atoms. However, the r.m.s.d. is only 0.73 Å when viperotoxin F and vipoxin are superimposed. The DbTx-A chain seems to be relatively more misaligned than DbTx-B when they are separately superimposed with the corresponding chains of viperotoxin F and vipoxin. This is evident from the r.m.s.d. values of 1.22 and 1.29 Å, respectively, for DbTx-A/RV-7 and DbTx-A/MER-INH superimpositions compared with r.m.s.d. values of 1.02 and 1.18 Å for DbTx-B/RV-4 and DbTx-B/MER-PLA_2 overlaps.

In DbTx, the two subunits are stabilized by a salt bridge between Asp49 of DbTx-A and Lys69 of DbTx-B. However, the equivalent salt bridge between Asp49 of DbTx-B and Lys69 of DbTx-A is not made. Furthermore, the interface area for DbTx is 584.1 $Å^2$, while those for viperotoxin F and vipoxin are 696.8 and 704.5 $Å^2$, respectively (calculated using the ClassPPi website; http://pre-s.protein.osaka-u.ac.jp/~classppi/index.html). In viperotoxin F and vipoxin reciprocating salt bridges (between Asp49 and Lys69 from both subunits) are formed. These results indicate that the interface interaction is weaker in DbTx compared with the other two toxins. This is also evident from Fig. 4, where the DbTx-B equivalent subunits of viperotoxin F and vipoxin (green and orange chains) align well with each other and are positioned closer to DbTx-A than is DbTx-B. The correlation between the subunit interaction and the pharmacological behaviour of these toxins are discussed in the next section.

The next important aspect of comparison is the calcium-binding loop. Normally, the PLA_2 subunit would undergo conformational change in order to bind to calcium. In some PLA_2s, the calcium-binding region is shown to contact inhi-

bitors (Schevitz *et al.*, 1995). Based on the Ca^{2+}-free structure of PLA_2 from *Crotalus atrox*, it has been suggested that the positively charged alkylammonium side chain of Lys69 may satisfy the need for partial charge neutralization in the region of the structurally shielded Asp49 carboxylate (Renetseder *et al.*, 1985; Brunie *et al.*, 1985).

The complete lack of activity of the inhibitor chain in vipoxin is explained by the replacement of the catalytically essential His48 by glutamine, whereas in the PLA_2 subunit residues His48, Tyr52 and Asp99 form an active site (Fig. 1) that is conserved in all PLA_2s. Comparison between the inhibitor chain of vipoxin and various PLA_2s shows a simi-

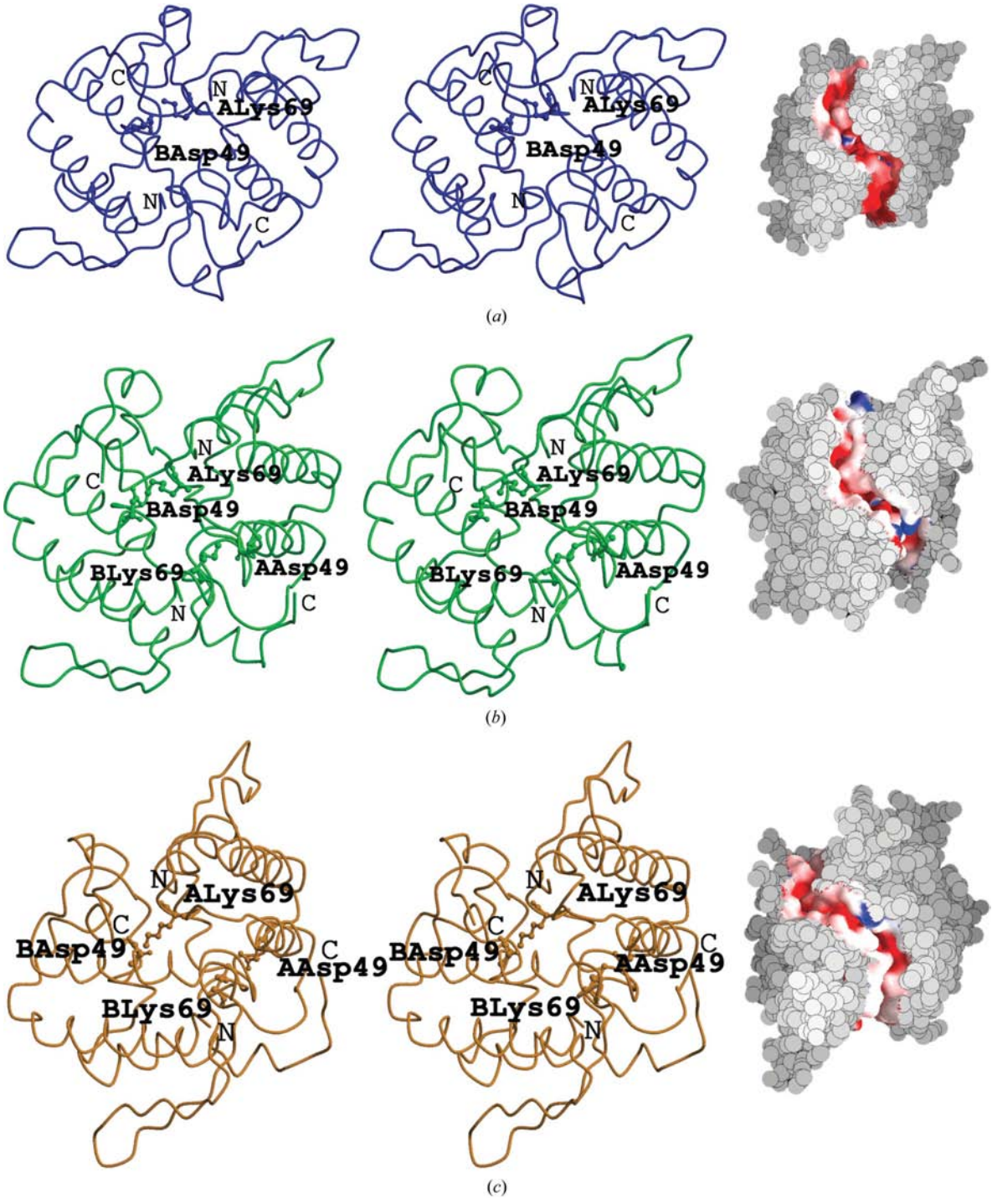

Figure 5
(*a*) Stereoview of the salt bridges (left panel) and the charge distribution (right panel) in the interface between the subunits of DbTx and those in (*b*) viperotoxin F and (*c*) vipoxin are shown. The molecules are coloured as in Fig. 4. The residues that are involved in the salt bridges between the subunits are labelled. The interface charge-distribution colours represent potentials from $-10k_BT^{-1}$ (red) to $+10k_BT^{-1}$ (blue). The orientations in all the panels are almost identical.

Table 3
Catalytic activity of the DbTx dimeric complex, of individual subunits A and B and of the complexes formed upon mixing the two subunits in various molar ratios.

A:B molar ratio	PLA_2 specific activity (μmol min^{-1} mg^{-1}), mean $\pm$ SD	Catalytic activity relative to DbTx-B† (%)
DbTx-B (PLA_2)	2110 $\pm$ 69	100
DbTx-A (inhibitor)	578 $\pm$ 10	27.4
DbTx dimeric complex	1377 $\pm$ 50	65.3 (35%)
DbTx-A + DbTx-B, 0.5:1	1793 $\pm$ 42	84.9 (15%)
DbTx-A + DbTx-B, 1:1	1421 $\pm$ 80	67.3 (32%)
DbTx-A + DbTx-B, 2:1	553 $\pm$ 30	29.2 (70%)
DbTx-A + DbTx-B, 4:1	460 $\pm$ 14	21.8 (78%)
DbTx-A + DbTx-B, 6:1	400 $\pm$ 30	19.1 (81%)
DbTx-A + DbTx-B, 8:1	358 $\pm$ 14	16.8 (83%)

† Values in parentheses denote the percentage inhibition of DbTx-B activity by DbTx.

larity in the region of the active centre. Except the Gln48 residue of vipoxin (which is His48 in DbTx-A, RV-7 and other PLA_2 chains), the other conserved residues Tyr52, Tyr73 and Asp99 form the same hydrogen-bond network as in mammalian and venom PLA_2s. Also, the same overlap is observed for the invariant hydrophobic side chains of the hydrophobic tunnel.

3.3. Comparison of toxicity and pharmacological effect

DbTx and viperotoxin F are presynaptic toxins, while vipoxin is a postsynaptic toxin (Mancheva *et al.*, 1987; Thwin *et al.*, 1996). Table 3 shows the catalytic activity of the individual subunits DbTx-A and DbTx-B, the naturally formed dimeric complex and the complexes formed upon mixing the two subunits in various molar ratios. The specific PLA_2 activity of DbTx-A (578 $\pm$ 10 μmol min^{-1} mg^{-1}) is only about 3.5-fold lower than that of catalytically active DbTx-B (2110 $\pm$ 69 μmol min^{-1} mg^{-1}). In contrast, the RV-7 inhibitor subunit has a 100-fold lower catalytic activity than that of RV-4, the equivalent of DbTx-B (Wang *et al.*, 1992). In vipoxin the inhibitor chain is completely inactive (Aleksiev & Tchorbanov, 1976) owing to the His48 mutation, as explained in §3.2.

The effect of complex formation on the enzyme activity of DbTx-B and inhibition by DbTx-A (Table 3) shows that only about 30% of the enzyme activity of DbTx-B is inhibited by DbTx-A upon formation of the dimeric complex in a unimolar ratio, while about 50% of RV-4 enzyme activity is reduced by RV-7 at the same molar ratio (Wang *et al.*, 1992). Moreover, the IC_{50} value calculated from the sigmoidal inhibition curve (Fig. 2*b*) further indicates that 1.42 *M* DbTx-A inhibitor is required to reduce DbTx-B (1 *M*) to half of its initial catalytic activity, while an equal molar ratio of RV-7 to RV-4 (1:1) is sufficient to inhibit the catalytic activity of RV-4 to 50% of its original catalytic activity (Wang *et al.*, 1992), thus suggesting that DbTx-A is a weaker inhibitor of DbTx-B than RV-7 is of RV-4.

Mice that were intraperitoneally injected with DbTx-B (or its complex with DbTx-A) showed neurotoxic symptoms, such as hind-limb paralysis, convulsions and respiratory distress. The lethal (intraperitoneal) dose of DbTx-B is estimated to be 0.5 μg g^{-1}, while that of the dimeric complex (DbTx-A–DbTx-B) is about 0.1 μg g^{-1}. Although DbTx-A alone is nonlethal, even at doses as high as 1.5–2 μg g^{-1}, it increases the lethal potency of DbTx-B by about fivefold after the A and B subunits form a complex in a unimolar ratio. This potentiating effect of the DbTx-A inhibitor is thus similar to that of the RV-7 inhibitor, while it is different to that of the vipoxin inhibitor, which decreases the toxicity of its counterpart PLA_2 subunit by fivefold.

4. Discussion

We have isolated a PLA_2 toxin termed daboiatoxin (DbTx) from the venom of the Burmese Russell's viper (*D. russelli siamensis*). It is oedematogenic and produces neurotoxic symptoms in mice. It exhibits indirect haemolytic activity and a strong myonecrotic activity and is cytotoxic. The amino-acid sequence of DbTx shows a significant resemblance to those of viperotoxin F from the Taiwan Russell viper (*D. russelli formosensis*) and vipoxin from the Bulgarian viper (*V. ammodytes ammodytes*). In a previous study (Thwin *et al.*, 1995), DbTx was reported to be a monomeric PLA_2 molecule. However, further chromatographic separation using C_{18} reverse-phase HPLC in the present study has resolved DbTx into two separate chains, both of 122 amino-acid residues in length. The two PLA_2 chains readily associate in solution to form a dimeric molecule as indicated by gel filtration as well as dynamic light-scattering experiments. The PLA_2 enzymatic activity of both chains has been measured using the secretory PLA_2 assay kit. Similar to the neurotoxic viperotoxin F complex (RV-7–RV-4; Wang *et al.*, 1992), DbTx is a complex between two PLA_2 chains. The lethal activity of the two chains has also been studied in male albino mice. Chain A is a less lethal acidic PLA_2 with lower PLA_2 activity like RV-7, while chain B is an enzymatically active basic PLA_2 that is similar to RV-4. Both components of DbTx are highly homologous proteins and their amino-acid sequences share 65% identity. Chain A reduces the enzymatic activity of DbTx chain B by 30% of its original activity, thus indicating that like the vipoxin inhibitor and RV-7, DbTx chain A acts as an inhibitor, decreasing the enzymatic activity of DbTx chain B.

We thank the Academic Research Fund, National University of Singapore for funding support to PG and KS.

References

Aleksiev, B. & Tchorbanov, B. (1976). *Toxicon*, **14**, 477–485.
Banumathi, S., Rajashankar, K. R., Notzel, C., Aleksiev, B., Singh, T. P., Genov, N. & Betzel, C. (2001). *Acta Cryst.* D**57**, 1552–1559.
Brünger, A. T., Adams, P. D., Clore, G. M., DeLano, W. L., Gros, P., Grosse-Kunstleve, R. W., Jiang, J.-S., Kuszewski, J., Nilges, M., Pannu, N. S., Read, R. J., Rice, L. M., Simonson, T. & Warren, G. L. (1998). *Acta Cryst.* D**54**, 905–921.
Brunie, S., Bolin, J., Gewirth, D. & Sigler, P. B. (1985). *J. Biol. Chem.* **260**, 9742–9749.
Chandra, V., Kaur, P., Jasti, J., Betzel, C. & Singh, T. P. (2001). *Acta Cryst.* D**57**, 1793–1798.

Chandra, V., Kaur, P., Srinivasan, A. & Singh, T. P. (2000). *J. Mol. Biol.* **296**, 1117–1126.
Chandra, V., Nagpal, A., Srinivasan, A. & Singh, T. P. (1999). *Acta Cryst.* D**55**, 925–926.
Collaborative Computational Project, Number 4 (1994). *Acta Cryst.* D**50**, 760–763.
Hooft, R. W. W., Vriend, G., Sander, C. & Abola, E. E. (1996). *Nature (London)*, **381**, 272.
Huang, H. C. & Lee, C. Y. (1984). *Toxicon*, **22**, 207–217.
Jones, T. A., Zou, J.-Y., Cowan, S. W. & Kjeldgaard, M. (1991). *Acta Cryst.* A**47**, 110–119.
Kraulis, P. J. (1991). *J. Appl. Cryst.* **24**, 946–950.
Laskowski, R. A., MacArthur, M. W., Moss, D. S. & Thornton, J. M. (1993). *J. Appl. Cryst.* **26**, 283–291.
Lok, S. M., Rong, G., Rouault, M., Lambeau, G., Gopalakrishnakone, P. & Swaminathan, K. (2005). *FEBS J.* **272**, 1211–1220.
Mancheva, I., Kleinschmidt, T., Aleksiev, B. & Braunitzer, G. (1987). *Biol. Chem. Hoppe-Seyler*, **368**, 343–352.
Merritt, E. A. & Bacon, D. J. (1997). *Methods Enzymol.* **277**, 505–524.
Otwinowski, Z. & Minor, W. (1997). *Methods Enzymol.* **276**, 307–326.
Perbandt, M., Tsai, I. H., Fuchs, A., Banumathi, S., Rajashankar, K. R., Georgieva, D., Kalkura, N., Singh, T. P., Genov, N. & Betzel, C. (2003). *Acta Cryst.* D**59**, 1679–1687.
Perbandt, M., Wilson, J. C., Eschenburg, S., Mancheva, I., Aleksiev, B., Genov, N., Willingmann, P., Weber, W., Singh, T. P. & Betzel, C. (1997). *FEBS Lett.* **412**, 573–577.
Renetseder, R., Brunie, S., Dikstra, B. W., Drenth, J. & Sigler, P. B. (1985). *J. Biol. Chem.* **260**, 11627–11634.
Schevitz, R. W., Bach, N. J., Carlson, D. G., Chirgadze, N. Y., Clawson, D. K., Dillard, R. D., Draheim, S. E., Hartley, L. W., Jones, N. D., Mihelich, E. D., Olkowski, J. L., Snyder, D. W., Sommers, C. & Wery, J. P. (1995). *Nature Struct. Biol.* **2**, 458–465.
Shatsky, M., Nussinov, R. & Wolfson, H. J. (2002). *Lecture Notes Comput. Sci.* **2452**, 235–250.
Thwin, M. M., Gopalakrishnakone, P., Yuen, R. & Tan, C. H. (1995). *Toxicon*, **33**, 63–76.
Thwin, M. M., Gopalakrishnakone, P., Yuen, R. & Tan, C. H. (1996). *Toxicon*, **34**, 183–199.
Tsai, I. H., Lu, P. J. & Su, J. C. (1996). *Toxicon*, **34**, 99–109.
Vagin, A. & Teplyakov, A. (1997). *J. Appl. Cryst.* **30**, 1022–1025.
Wang, Y. M., Lu, P. J., Ho, C. L. & Tsai, I. H. (1992). *Eur. J. Biochem.* **209**, 635–641.
Warrell, D. A. (1989). *Trans. R. Soc. Trop. Med. Hyg.* **83**, 732–740.
Warrell, D. A., Phillips, R. E., Theakston, D. G., Galigeoara, Y., Abeysekera, D. T., Dissanayake, P., Hutton, R. A. & Aloysius, D. J. (1989). *Toxicon*, **27**, 85–85.
Wuster, W., Otsuka, S., Malhotra, A. & Thorpe, R. S. (1992). *Biol. J. Linn. Soc.* **47**, 97–113.